

## Fast Track Communication

# Phase-resolved measurement of electric charge deposited by an atmospheric pressure plasma jet on a dielectric surface

R Wild<sup>1</sup>, T Gerling<sup>2</sup>, R Bussiahn<sup>2</sup>, K-D Weltmann<sup>2</sup> and L Stollenwerk<sup>1</sup><sup>1</sup> Institute for Physics, University of Greifswald, Felix-Hausdorff-Str. 6, 17487 Greifswald, Germany<sup>2</sup> Leibniz Institute for Plasma Science and Technology (INP Greifswald), Felix-Hausdorff-Str. 2, 17489 Greifswald, GermanyE-mail: [wild@physik.uni-greifswald.de](mailto:wild@physik.uni-greifswald.de), [gerling@inp-greifswald.de](mailto:gerling@inp-greifswald.de) and [stollenwerk@physik.uni-greifswald.de](mailto:stollenwerk@physik.uni-greifswald.de)

Received 6 November 2013, revised 19 November 2013

Accepted for publication 22 November 2013

Published 20 December 2013

**Abstract**

The surface charge distribution deposited by the effluent of a dielectric barrier discharge driven atmospheric pressure plasma jet on a dielectric surface has been studied. For the first time, the deposition of charge was observed phase resolved. It takes place in either one or two events in each half cycle of the driving voltage. The charge transfer could also be detected in the electrode current of the jet. The periodic change of surface charge polarity has been found to correspond well with the appearance of ionized channels left behind by guided streamers (bullets) that have been identified in similar experimental situations. The distribution of negative surface charge turned out to be significantly broader than for positive charge. With increasing distance of the jet nozzle from the target surface, the charge transfer decreases until finally the effluent loses contact and the charge transfer stops.

Keywords: plasma jet, surface charge, guided streamer


(Some figures may appear in colour only in the online journal)

Atmospheric pressure plasma jets (APPJs) are well-established plasma sources in applications such as surface treatment or decontamination of biological surfaces. Because of their effluent, they can be applied without confining the plasma between electrodes [1]. Therefore, and due to its low gas temperature, the application of APPJs in the medical sector increasingly gained attention [2].

In this contribution we present a spatially and phase resolved measurement of electric charge being deposited by an APPJ on a dielectric surface. The measurement takes

advantage of the electro-optic property of the used surface material ( $\text{Bi}_{12}\text{SiO}_{20}$ , short BSO), which becomes birefringent in the presence of an electric field. This technique is well-known for the quantification of surface charge distributions in dielectric barrier discharges [3, 4], but has, to the best of our knowledge, never been applied to an APPJ effluent.

In order to measure the deposited charge on the BSO surface, the state of polarization of a pre-defined incident light beam is evaluated (see figure 1(b)). Therefore, an LED light beam ( $\lambda = 638 \text{ nm}$ , FWHM: 10 nm) with linear polarization is prepared. On its way from the beam splitter, being reflected by the grounded aluminum mirror behind the BSO crystal, and finally through an analyser to the camera, it is retarded by twice the phase retardation from the  $\lambda/8$ -wave plate and the

 Content from this work may be used under the terms of the [Creative Commons Attribution 3.0 licence](https://creativecommons.org/licenses/by/3.0/). Any further distribution of this work must maintain attribution to the author(s) and the title of the work, journal citation and DOI.

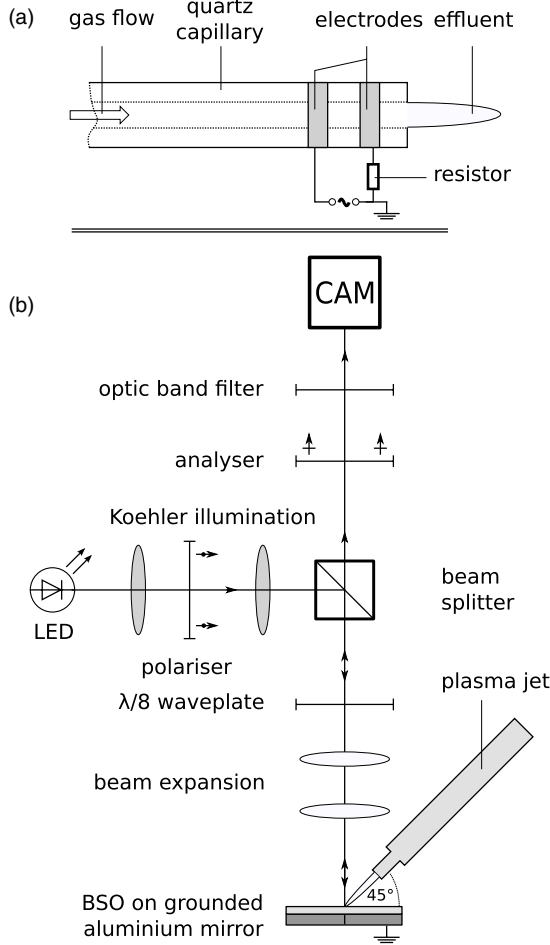


**Figure 1.** Sketch of the experimental set-up. (a) The plasma jet consisting of a quartz capillary. The electrodes are wrapped around the capillary. (b) Set-up for the measurement of surface charges on the BSO crystal.

additional phase shift  $\Delta\Phi$  according to the voltage drop  $U_{\text{BSO}}$  over the BSO crystal, with

$$\Delta\Phi = 2\pi \lambda^{-1} n_0^3 r_{41} U_{\text{BSO}}. \quad (1)$$

In equation (1),  $n_0$  is the undisturbed refraction index ( $n_0 = 2.54$ ) of BSO, and  $r_{41}$  is its electro-optic constant ( $r_{41} = 5.3 \text{ pmV}^{-1}$ ).

The analyser in front of the high speed camera (Phantom Miro) is orientated perpendicular to the initial polarizer and results in an intensity profile  $I(x, y)$  describing the surface charge distribution. An optic band filter in front of the camera ensures that only the light from the LED is detected.

The charge density  $\sigma$  on the substrate surface is calculated via the ratio  $I(x, y)/I_0(x, y)$ .  $I_0(x, y)$  is a reference camera image recorded without any charge distribution on the BSO surface.  $\sigma$  is determined via

$$\sigma(x, y) = \frac{\varepsilon_0 \varepsilon_{\text{BSO}}}{a_{\text{BSO}}} \cdot \frac{\lambda}{4\pi n_0^3 r_{41}} \left( \frac{I(x, y)}{I_0(x, y)} - 1 \right), \quad (2)$$

with a thickness of the BSO crystal of  $a_{\text{BSO}} = 0.7 \text{ mm}$ , an dielectric constant of BSO of  $\varepsilon_{\text{BSO}} = 56$ , and  $\varepsilon_0$  being the vacuum permittivity. A more detailed description of the optical

set-up and the corresponding derivation of equation (2) are given in [4].

The spatial resolution of the surface charge measurement is determined by the thickness  $a_{\text{BSO}}$  of the BSO crystal and thus  $0.7 \text{ mm}$ . The life time of charges is in the order of seconds [5], so charge decay is not relevant for these measurements. In order to achieve a temporal resolution of the charge measurement, the LED works in a pulsed operation mode. The pulses have a duration of  $500 \text{ ns}$  and can be phase shifted relative to the supply voltage of the jet. Overview measurements have been done with a temporal resolution of  $\Delta t = 4.2 \mu\text{s}$ . Times of interest, such as the change of polarity, have been observed with a temporal resolution of  $\Delta t = 0.6 \mu\text{s}$ .

The plasma jet (see figure 1(a)) consists of a quartz capillary with an inner diameter of  $0.5 \text{ mm}$  and a wall thickness of  $1 \text{ mm}$ . The plasma is generated between two ring electrodes ( $2 \text{ mm}$  width each) that are wrapped around the capillary in a distance of  $5 \text{ mm}$  from each other and  $2 \text{ mm}$  from the jet nozzle. An external sinusoidal voltage of  $8 \text{ kV}_{\text{pp}}$  is applied at a frequency of  $13 \text{ kHz}$ . The current through the front ring electrode is measured over a series resistor ( $R = 100 \Omega$ ). Hence, the potential of the front electrode is close to ground. The effluent is produced using a static helium gas flow of  $3 \text{ slm}$  through the capillary. If not mentioned otherwise, the plasma effluent has a length of  $2.6 \text{ mm}$  and is hence in contact with the BSO surface. To avoid the plasma jet obscuring the view of the camera, it is aligned at an angle of  $45^\circ$  to the surface. The whole set-up is operated without further housing at atmospheric pressure in ambient air.

In figure 2, the applied voltage, electrode current, and the mean charge density of the observed area are shown. To interpret this figure, one has to keep in mind the dynamics of ‘guided streamers’ (or ‘plasma bullets’) that form the effluent of a plasma jet: in the presence of a grounded target in front of the nozzle, they may propagate forward or backward relative to the gas flow [6, 7]. In the negative current half wave ( $0\text{--}38.5 \mu\text{s}$ , see figure 2), two current peaks are visible, each one followed by a small reverse current peak. The main peaks are interpreted as barrier discharge events between the electrodes, which are followed by the propagation of a guided streamer from the BSO surface towards the capillary (‘reverse bullet’) [7]. In the positive half wave ( $38.5\text{--}77 \mu\text{s}$ ) a single current peak is visible, again followed by a small reverse current peak. Again, the main peak results from the barrier discharge, this time followed by a ‘forward’ bullet [7]. In both cases, when the streamer reaches the respective counter electrode, it produces a channel with high conductivity between the capillary and the BSO crystal surface [8]. As will be seen below, through these channels a charge transfer to the surface takes place which results in the small reverse current peaks.

The lower part of figure 2 correlates the mean deposited charge density and the electrical current. During one period of the driving voltage, both positive and negative charges are deposited on the BSO crystal. Significant events are the deposition of positive charges (at  $60\text{--}70 \mu\text{s}$  in figure 2), and the deposition of negative charges (at  $25\text{--}45 \mu\text{s}$ ), which contrary to the first mentioned deposition is a two-step process due to the two discharge events.

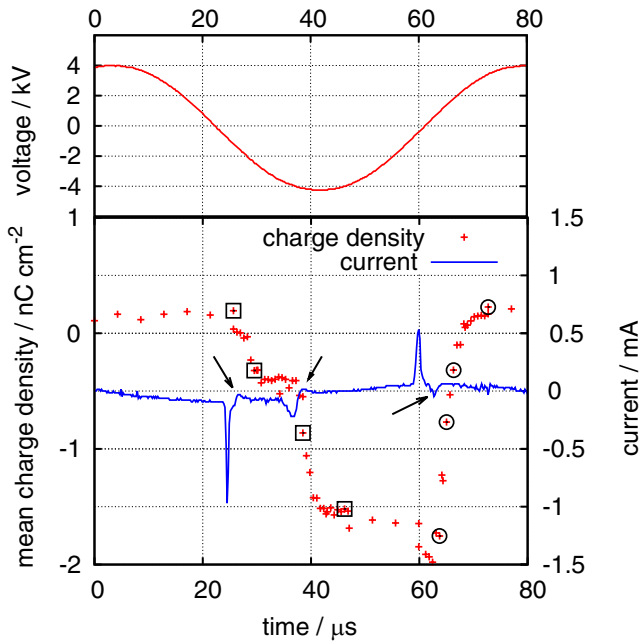


**Figure 2.** Temporal evolution of the applied voltage, the electrode current and the mean surface charge on the crystal surface. □—selected times in figure 4. ○—selected times in figure 5. The arrows indicate reverse current peaks.

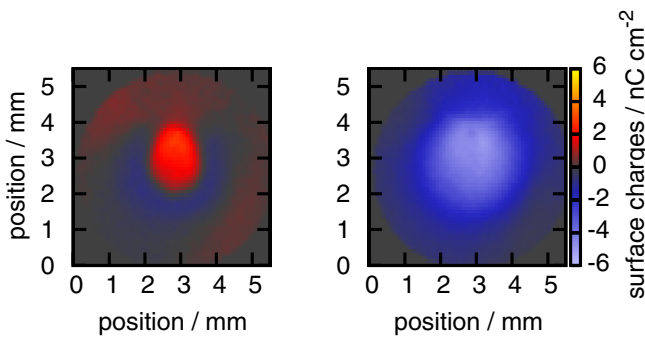


**Figure 3.** Surface charge distribution for positive (left) and negative (right) polarity. The measurements are taken at  $t = 12.8 \mu\text{s}$  (left) and  $t = 55.6 \mu\text{s}$  (right), when the charge density is temporally constant.

The spatial surface charge distributions are shown for both polarities in figure 3. The effluent of the plasma jet hits the displayed area from the top. Due to its tilt relative to the crystal surface, the surface charge spots are elliptically deformed. With respect to their polarity, the surface charge distributions exhibit a significant asymmetry in peak charge density and the occupied area. The maximum positive charge density is  $\hat{\sigma}_{\text{pos}} = 2 \text{ nC cm}^{-2}$ . The area is assumed to be elliptical and its boundaries are defined as the points of inflection in their charge profile. In the positive case an area of  $A_{\text{pos}} = 2.8 \text{ mm}^2$  is determined. The negative charge density has a maximum absolute value of  $\hat{\sigma}_{\text{neg}} = 4.8 \text{ nC cm}^{-2}$  and occupies an area of  $A_{\text{neg}} = 8.2 \text{ mm}^2$ , which is 2.9 times larger than in the positive case. Thus, negative charges partly survive the deposition of positive charges as a ring around the positively charged area. Consequently, as seen in figure 2, the mean charge density on the BSO surface is shifted towards negative values.

The phenomenon of a broader distribution of the negative charge compared to the positive one also has been observed frequently for planar barrier discharges, e.g. [3, 4]. From numerical simulations [9] it is known that the electric field close to the surface develops a large lateral component due to the accumulating surface charges. Thus, charge carriers approaching the surface in the end of a discharge drift to the sides. Due to their much larger mobility, this effect is more pronounced for electrons than for ions.

The charge deposition process for positive charges on a negative background from 63.6 to 72.7  $\mu\text{s}$  is shown in figure 4. Negative charge is replaced by positive charge starting from the point where the effluent hits the BSO surface. The replacement area then grows downwards, along the direction of the plasma jet tilt. Note that the charge deposition process is much slower ( $\approx 10 \mu\text{s}$ ) than expected from the impact of a guided streamer (hundreds of nanoseconds [7]). This leads to the assumption that the observed phenomenon is the result of charge transportation through the conducting channel from the crystal surface to the jet nozzle that has been left behind by the ionization wave.

In figure 5, the deposition of negative charge on a positive background in the time range from 25.5 to 46.1  $\mu\text{s}$  is shown. The significant difference to the previously described charging process is that the charge reversal requires two guided streamers to complete the process. Within the first 4  $\mu\text{s}$ , the positive charges are neutralized, leaving behind only the ring of negative charges (see  $t = 29.8 \mu\text{s}$ ). Approximately at  $t = 39.5 \mu\text{s}$ , a second reverse bullet is launched, in whose aftermath the BSO surface is negatively charged. Within the next few microseconds, the deposition of negative charge continues so that the density profile closes up continuously with the ring of deposited charges. Note that according to figure 2(b), the absolute value of transported charge in the positive half wave is exactly the same as in the negative half wave.

Furthermore, the influence of the nozzle-surface distance on the deposited charge is investigated. Three regions can be distinguished: at small distances ( $d < 9 \text{ mm}$ ) the effluent is bent towards the BSO crystal and is in touch with it. At large distances ( $d > 10 \text{ mm}$ ) the entire effluent is parallel to the initial gas flow and does not touch the crystal surface; the reverse current peaks seen in figure 2 disappear. At intermediate distances the two operation modes alternate frequently, thus surface charge measurements are not reliable. In figure 6, for various distances a horizontal profile of the surface charge distribution at  $y = 3 \text{ mm}$  is shown. Up to intermediate distances, the peak charge density is reduced as the distance is increased. For large distances, the surface charge density is close to zero. In conclusion, the mechanism of charge deposition is as follows: in the free effluent, i.e. with the target being far away from the nozzle, charge carriers recombine within a few millimetres (here within  $d \approx 10 \text{ mm}$ ). Thus, no charges can be deposited on the target. However, if the target is close enough to the nozzle, guided streamers emerging from the jet hit the target and the remaining conductive plasma channel allows for a charge transfer. The increased resistivity of long plasma channels (both due to the bare length and due

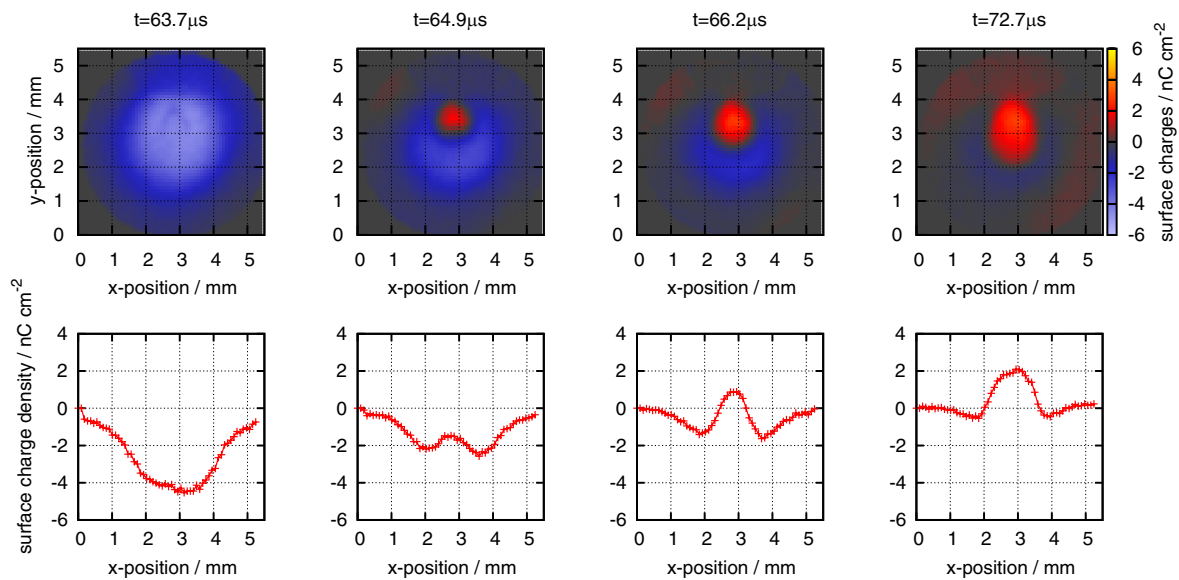


**Figure 4.** Top row: spatially resolved surface charge distributions at selected times in the negative current half wave. Bottom row: horizontal profiles along  $y = 3\text{ mm}$  in the corresponding surface charge distribution.

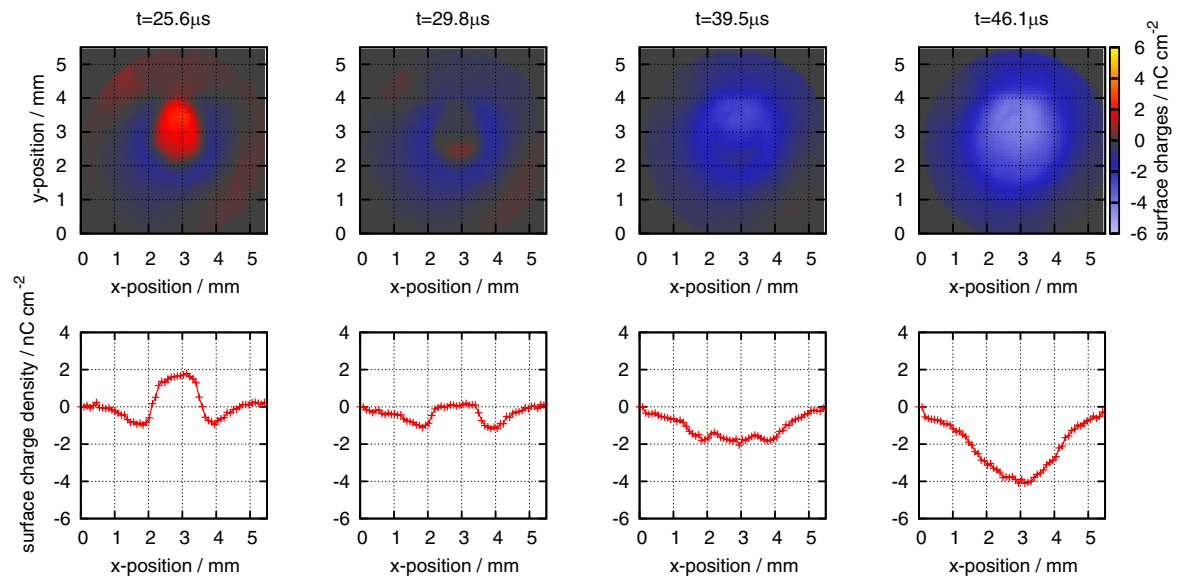


**Figure 5.** Top row: spatially resolved surface charge distributions at selected times in the positive current half wave. Bottom row: horizontal profiles along  $y = 3\text{ mm}$  in the corresponding surface charge distribution.

to the decreasing charge carrier density in the initiating guided streamer) lead to a decreased amount of transferred charge. The electric field deformation resulting from both the grounded target and the deposited surface charge lead to a bending of the effluent and allow for the formation of additional reverse bullets starting from the target surface.

Results presented in this article might help to understand effects of plasma jets in interaction with surfaces, like etching [10], or its application in the medical sector. In [11] the authors point out that knowledge on quantity and behaviour of physical properties like electrical charges in plasma sources is crucial for its application on living tissue. In the present work, space and phase resolved charge density distributions on a dielectric surface (BSO) are presented. The reversals of charges are strongly correlated with the ignition of guided streamers, which were identified by current signals. The

timescale of charge exchange exceeds the time of expected streamer impact time. Hence, the majority of charges is transported by the conducting channel which is left behind by the streamer. Negative charge carriers occupy an area almost three times larger than the positive ones. Thus, positive charges are always surrounded by residual negative surface charges. An increased distance from the plasma jet nozzle to the dielectric surface results in a decreased charge deposition. Finally, the jet loses contact with the target surface and no charge deposition takes place any more.

### Acknowledgments

The authors are grateful to Rüdiger Titze, Uwe Meissner and Peter Druckrey for providing practical and technical

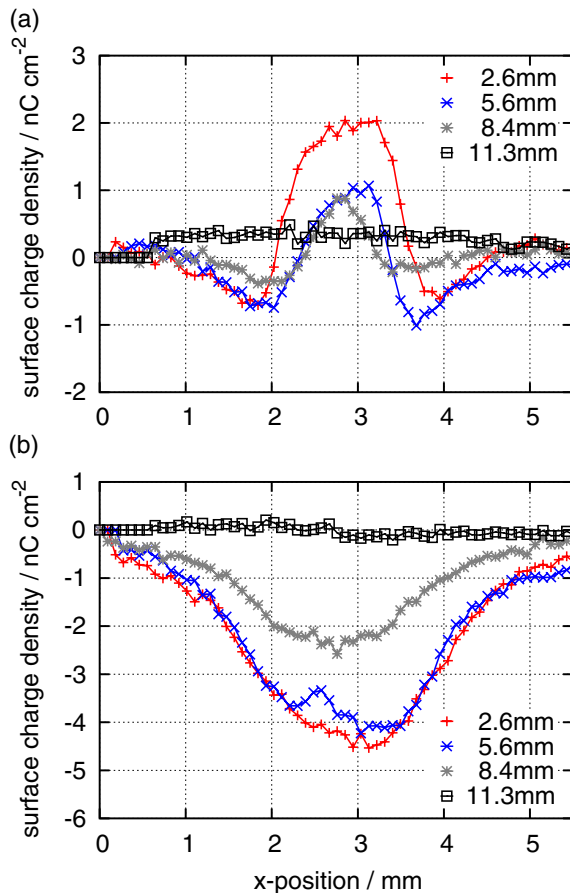


**Figure 6.** Horizontal profiles of the surface charge distribution at  $y = 3$  mm for selected distances between jet nozzle and BSO surface, (a) after a complete deposition of positive charges, (b) after a complete deposition of negative charges.

assistance. This work was funded by the *Deutsche Forschungsgemeinschaft* SFB TRR-24 (B14) and by the multi-disciplinary research cooperation, *Campus PlasmaMed*, supported by German Ministry of Education and Research (BMBF, grant no 13N11188).

## References

- [1] Lu X, Laroussi M and Puech V 2012 On atmospheric-pressure non-equilibrium plasma jets and plasma bullets *Plasma Sources Sci. Technol.* **21** 034005
- [2] Weltmann K-D, Kindel E, Brandenburg R, Meyer C, Bussiahn R, Wilke C and von Woedtke Th 2009 Atmospheric pressure plasma jet for medical therapy: plasma parameters and risk estimation *Contrib. Plasma Phys.* **49** 631–40
- [3] Stollenwerk L, Laven J G and Purwins H-G 2007 Spatially resolved surface-charge measurement in a planar dielectric-barrier discharge system *Phys. Rev. Lett.* **98** 255001
- [4] Bogaczyk M, Wild R, Stollenwerk L and Wagner H-E 2012 Surface charge accumulation and discharge development in diffuse and filamentary barrier discharges operating in He, N<sub>2</sub> and mixtures *J. Phys. D: Appl. Phys.* **45** 465202
- [5] Wild R, Benduhn J and Stollenwerk L 2013 Lifetime of surface charges on BSO in barrier discharges *Conf. Proc. 31 ICPiG (Granada, Spain, July, 2013)*
- [6] Nastuta A F, Topala I and Popa G 2011 Iccd imaging of atmospheric pressure plasma jet behavior in different electrode configurations *IEEE Trans. Plasma Sci.* **39** 2310
- [7] Gerling T, Nastuta A V, Bussiahn R, Kindel E and Weltmann K-D 2012 Back and forth directed plasma bullets in a helium atmospheric pressure needle-to-plane discharge with oxygen admixtures *Plasma Sources Sci. Technol.* **21** 034012
- [8] Shashurin A, Shneider M N and Keidar M 2012 Measurements of streamer head potential and conductivity of streamer column in cold nonequilibrium atmospheric plasmas *Plasma Sources Sci. Technol.* **21** 034006
- [9] Stollenwerk L, Amiranashvili Sh, Boeuf J-P and Purwins H-G 2007 Formation and stabilisation of single current filaments in planar dielectric barrier discharge *Eur. Phys. J. D* **44** 133–9
- [10] Fricke K, Steffen H, von Woedtke T, Schröder K and Weltmann K-D 2011 High rate etching of polymers by means of an atmospheric pressure plasma jet *Plasma Process. Polym.* **8** 51–8
- [11] von Woedtke Th, Reuter S, Masur K and Weltmann K-D 2013 Plasmas for medicine *Phys. Rep.* **530** 291–320